A CALCULATION OF POSITRON SOURCE YIELDS*

M.B.James, R.H.Miller and B.M.Woo

Stanford Linear Accelerator Center
Stanford University, Stanford, California 94305 USA

Coil Redesign

On June 28, 1976 the high field coil of the SLAC positron source failed with a short to the ground. The spare failed after a few weeks of operation, when it developed a water leak at a brazed joint on a mitered bend in the interior of the coil. A third coil assembly, manufactured from salvaged pancakes and conductor from the first two assemblies, has run satisfactorily since. We decided to investigate some design changes to make the coil more conservative. The goals for the new design were:

1. to eliminate the internal brazed joints in the conductor,
2. to improve the iron configuration in order to achieve equal or higher field with reduced current density, and
3. to reduce the power consumption of the coil.

The new coil is now under construction and will be installed next spring. The original and new designs are shown in Fig. 1a,b, respectively. Removing the inner coil and replacing it with iron increased the field at the target, while reducing the total amp turns 25%. Additional iron outside the coil further increased the efficiency of the coil. Two alternates of the new design have been considered. The first (new 4-coil) has only coil pancakes 1, 2, 3, and 4 shown in Fig. 1b. The second (new 6-coil) has all six pancakes. Table I

Table I. High Field Coil Parameters

	Original	New 4-coil	New 6-coil
Turns	206	120	180
Current	3250	3170	3170
Amp turns	669,500	380,400	570,600
Field at target	16.3 kG	17.7 kG	20.6 kG
Current density	28.9 A/mm^2	26.6 A/mm^2	26.6 A/mm^2
Power	388 kW	294 kW	441 kW

*Work supported by the Energy Research and Development Administration.

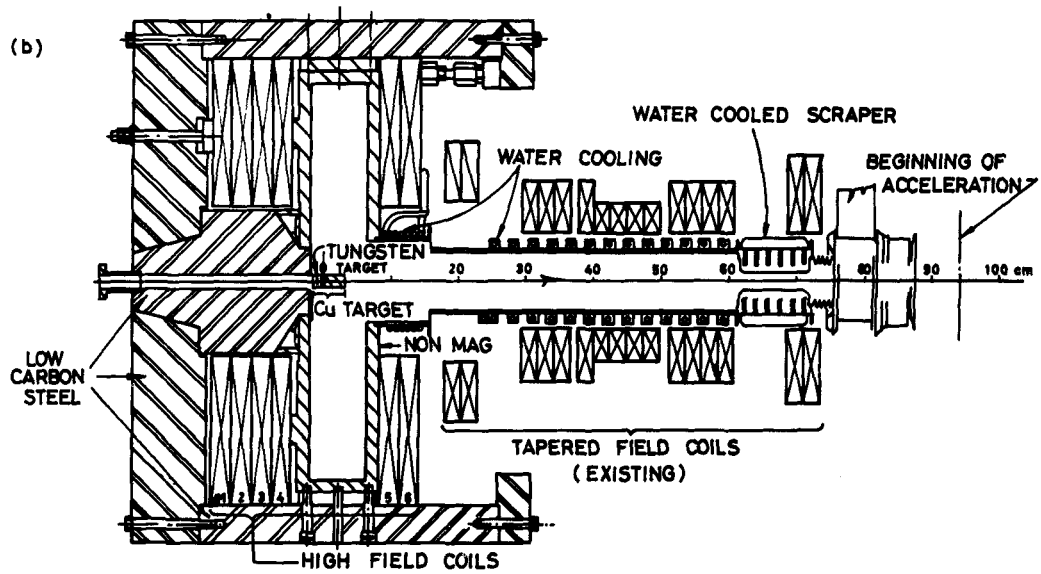

Fig. 1. (a) Present coil configuration. (b) New coil configuration.

summarizes the properties of the three coil configurations. Figure 2 shows the axial magnetic field for each of the three solenoid configurations.

The new coil design adheres to the adiabatic taper concept proposed by Helm[1,2] and embodied in the present coil. The new coil was designed by W. Brunk and K. Porzuczek of the SLAC Mechanical Engineering Department.

Monte Carlo Program

The distribution in phase space of secondary particles in the electromagnetic shower leaving the positron target was calculated using Ford and Nelson's Monte Carlo program EGS.[3] This program will calculate the shower development in arbitrary materials with arbitrary geometry from primary particles distributed arbitrarily in phase space. In this study we calculated the showers in copper and tungsten targets from zero radius primary electron beams at 80 MeV, 250 MeV, 1 GeV, and 7 GeV. The target thicknesses were chosen for shower maximum except for the 7 GeV runs where the thicknesses were those actually used at SLAC.

The Monte Carlo program output lists each incident particle, then lists the secondary particles from that incident particle. The program lists the following information for each particle: E = total energy; x, y, z = the rectangular position coordinates of the particle; u, v, w = the direction cosines of the particle momentum vector, relative to the x, y and z axes, respectively; q = -1, 0, 1 the charge on the particle, identifying it as an electron, photon or positron, respectively; and code—which distinguishes the primary particle from the secondary particle, and tells why the program ceased to track the particle (e.g., when the particle has reached the downstream face of the target). A program called "SORT" was written to use the output of the Monte Carlo program. SORT tests each secondary electron and positron which reaches the downstream face of the target, to see whether they fall within the admittance ellipsoid of each of the coil configurations.

Ray Tracing Program

We used Herrmannsfeldt's Electron Trajectory Program[4] to simulate the key positron trajectories through each of the four magnetic field configurations. The program uses relativistic equations of motion to calculate electron trajectories. We were interested in observing the positron trajectories in 3 field regions, the adiabatically tapered field, the uniform solenoid, and the fringe field at the end of the uniform solenoid. We simulated the first 3 meters of the 7-meter uniform solenoid. This does not give the same final Larmor phase as that of the 7-meter solenoid. The positron trajectories were calculated at 2.5 MeV intervals. Such large steps means that every Larmor phase is represented within each step at different energies. The uncertainty inherent in such large steps makes academic the problem of properly calculating the Larmor phase. We simulated the radial fields at the end of the uniform solenoid with a linearly decreasing magnetic segment 8 cm long. Although this is only a crude approximation, it gives us some idea of the behavior of the positrons in the fringing fields.

Admittance Ellipsoid Transformation

In order to calculate the positron yield it is necessary to calculate the admittance of the positron focusing systems. Helm[2] has calculated the admittance of the quadrupole focusing system downstream of the solenoid. The x, p_x and y, p_y plane intercepts are well represented by erect ellipses centered on the coordinate system with semiaxes of 0.7 cm and .22 MeV/c. Since the x and y planes are not coupled in such a quadrupole focusing system, it follows that the admittance four ellipsoid is erect. Thus it can be represented by the equation

$$\frac{p_x^2 + p_y^2}{(.22\ \text{MeV/c})^2} + \frac{x^2 + y^2}{(0.7\ \text{cm})^2} = \frac{p_r^2 + p_\phi^2}{(.22\ \text{MeV/c})^2} + \frac{r^2}{(0.7\ \text{cm})^2} \leq 1 \qquad (1)$$

where p_ϕ is the azimuthal momentum. In order to transform this ellipsoid back to the positron radiator, we assumed that the effect of the solenoids could be represented by a linear transformation, and hence would map a central ellipsoid into a central ellipsoid. Therefore, the admittance of the input to the solenoid can be represented by the general equation for a central ellipsoid:

$$Ax^2 + Bxy + Cy^2 + Dp_x^2 + Ep_xp_y + Fp_y^2 + Gxp_x + Hxp_y + Iyp_x + Jyp_y \leq 1. \qquad (2)$$

The admittance ellipsoid of the quadrupole focusing system has a circular intercept in the x, y plane and the p_x, p_y plane. It follows from this fact and from the cylindrical symmetry of the solenoid that the admittance at the radiator must also be circular in the x, y and p_x, p_y planes. The following constraints can thus be placed on the coefficients:

$$B = E = 0\ , \qquad D = F \equiv 1/b^2\ , \qquad G = J \equiv 1/c\ ,$$
$$A = C \equiv 1/a^2\ , \qquad H = -I \equiv 1/d\ .$$

The admittance ellipsoid at the radiator can now be written with four constants:

$$\frac{x^2 + y^2}{a^2} + \frac{p_x^2 + p_y^2}{b^2} + \frac{xp_x + yp_y}{c} + \frac{xp_y - yp_x}{d} \leq 1\ . \qquad (3)$$

In cylindrical coordinates, which the ray tracing program uses, the equation is:

$$\frac{r^2}{a^2} + \frac{p_r^2 + p_\phi^2}{b^2} + \frac{rp_r}{c} + \frac{rp_\phi}{d} \leq 1\ . \qquad (4)$$

The four constants can be determined by running four particles through the ray tracing program. A particle with $p_r = p_\phi = 0$ permits determination of a^2, while one with r=0 yields b^2. Once these values are known, a particle originating in the r, p_r plane, but not near either axis, gives c. Similarly, a particle originating in the rp_ϕ plane permits calculation of d. For a point on the surface of the admittance ellipsoid with $p_T^2 \equiv p_r^2 + p_\phi^2 = 0$, Eq. (4) becomes $r^2/a^2 = 1$. However, since for a linear transformation the input and the output ellipsoids scale, we can pick any initial value r_i (for $p_T = 0$) and write

$$\frac{r_i^2}{a^2} = \frac{p_{Tf}^2}{(.22\ \text{MeV/c})^2} + \left(\frac{r_f}{.7\ \text{cm}}\right)^2\ ,$$

$$a^2 = \frac{r_i^2}{\frac{p_{Tf}^2}{(.22\ \text{MeV/c})^2} + \left(\frac{r_f}{.7\ \text{cm}}\right)^2} \qquad \text{for } p_{r_i} = 0,\ p_{\phi i} = 0\ , \tag{5}$$

where subscript i denotes initial values as the particle leaves the target, and subscript f denotes the final values where the particle leaves the solenoid. Similarly,

$$b^2 = \frac{p_{ri}^2}{\frac{p_{Tf}}{(.22\ \text{MeV/c})^2} + \frac{r_f^2}{(.7\ \text{cm})^2}} \qquad \text{for } r_i = 0\ . \tag{6}$$

When $p_\phi = 0$, Eq. (4) becomes for a point not on the surface of the ellipsoids:

$$\frac{r_i^2}{a^2} + \frac{p_{ri}^2}{b^2} + \frac{r_i p_{ri}}{c} = \left(\frac{r_f}{.7\ \text{cm}}\right)^2 + \left(\frac{p_{Tf}}{.22\ \text{MeV/c}}\right)^2\ .$$

And solving for c, and similarly for d, we find

$$c = \frac{r_i p_{ri}}{\left(\frac{r_f^2}{.7^2} + \frac{p_{Tf}^2}{.22^2}\right) - \left(\frac{r_i^2}{a^2} + \frac{p_{ri}^2}{b^2}\right)}\ , \qquad d = \frac{r_i p_{\phi i}}{\left(\frac{r_f^2}{.7^2} + \frac{p_{Tf}^2}{.22^2}\right) - \left(\frac{r_i^2}{a^2} + \frac{p_{\phi i}^2}{b^2}\right)}\ . \tag{7,8}$$

Having calculated coefficients a, b, c, and d for Eq. (4), we ray traced selected particles which originate on the surface of the admittance ellipsoid. The fact that these particles came out on the surface of the admittance ellipsoid of Eq. (1) for the quadrupole focusing system, verified that the assumption of linearity was correct for energies above 5 MeV. At 5 MeV and below, the paraxial approximation does not hold for transverse momenta of interest. The admittance is no longer truly ellipsoidal, but we approximated it with hyperellipsoid calculated using Eqs. (5) through (8). It was necessary to iterate since linear scaling did not work.

The coefficients are a function of the positron energy. They were calculated for 12 energy values from 2.5 MeV to 30 MeV for each of 4 magnetic field configurations shown in Fig. 2: (1) the present solenoid starting from the tungsten target, (2) the present solenoid starting from the copper target, (3) the new 4-coil configuration, and (4) the new 6-coil design. In addition, the admittance ellipsoids were calculated for a fifth configuration: an idealized quarter wave transformer solenoid designed for 5 MeV positrons. The field is 7.35 kG for 5.5 cm downstream of the target; then decreases linearly for 3 cm to 2.1 kG. As with the other field configurations, this uniform field extends for 3 m and then decreases linearly to 0 kG in 8 cm.

Results of Calculations

The radial momentum acceptance gives the best understanding of the performance of each field configuration. This is true because the distribution of positrons in radial momentum is very broad. The radial momentum acceptance for positrons leaving the target

at r=0 is plotted as a function of energy in Fig. 3 for the four coil configurations. The first property that strikes the eye is that the 3 "adiabatic tapers" are surely not adiabatic, since considerable structure appears in the acceptances. The acceptances remain large, however, over the entire range from 2.5 MeV to 30 MeV. Furthermore, the acceptances increase with increasing field at the target. The quarter wave transformer behaves as expected with a large acceptance over only a narrow energy band centered 5 MeV. The 3/4 λ acceptance peak does not show because our calculation did not go low enough in energy.

In Fig. 4 we present the positron distributions in r, p_T, and E for 7 GeV electrons incident on 5 cm of copper and 1.9 cm of tungsten. These target thicknesses, which are slightly less than shower maximum, were found experimentally to be optimum with our present coil. The differential distribution function $\frac{dN}{dr}(r)$ falls to roughly half its maximum value at a radius of 1.2 mm for tungsten and at about 1.5 mm for copper. The incident beam had zero radius. For a finite incident beam radius this distribution must surely vanish at r=0 and rise linearly for small r. The positron distribution in transverse momentum for the copper target reaches a maximum value at about 2 MeV/c and remains constant out to 3 MeV/c while for tungsten it is still rising at 3 MeV/c. Thus the positrons leave the tungsten target in a smaller spot but with larger transverse momentum p_T.

The outputs from the Monte Carlo runs were sorted to find the number of electrons and positrons which fall within the admittance hyperellipsoids for each of the coil configurations. The results are presented as percentage yields in Table II. The new coil with 4 pancakes, which uses 24% less power, gives a 26% larger yield than the present coil. If we increase from 4 pancakes to 6 pancakes and hence increase the power consumption by 50%, we gain only 6% in e^+ yields. Clearly the 4 coil design is more reasonable.

Table II. Calculated Yields

	e^- Yield (%)	e^+ Yield (%)
Present coil : Cu target	12.0 ± .7	6.9 ± .5
Present coil : W target	26.2 ± 1.1	16.1 ± .8
New 4 coil : W target	33.5 ± 1.1	20.3 ± .9
New 6 coil : W target	35.5 ± 1.1	21.5 ± .9
Quarter wave: W target	11.1 ± .7	7.1 ± .5

It is useful to compare the calculated results with the experimental results with the present coil. The best observed yield with a tungsten target is 12%, as compared with the calculated yield for the present coil of 16.1%. It is entirely reasonable that misalignments may reduce the actual 4 dimensional admittance by 25% below the theoretical value. A few years ago a careful experimental comparison of the positron yield from copper and from tungsten was made. The yield from copper was 40% of the yield from tungsten, in reasonable agreement with the calculated value of 43%.

The positron yields for our present coil were calculated for various incident electron energies from 7 GeV to 80 MeV and are tabulated in Table III. The positron yield divided

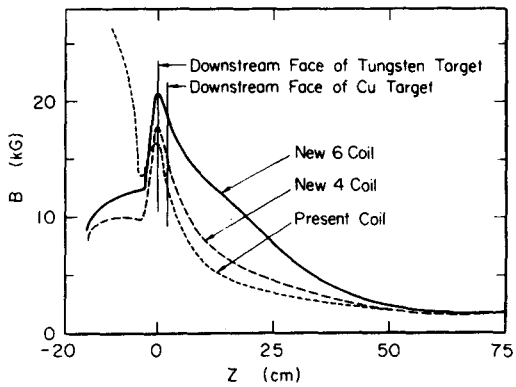

Fig. 2. Calculated axial magnetic fields.

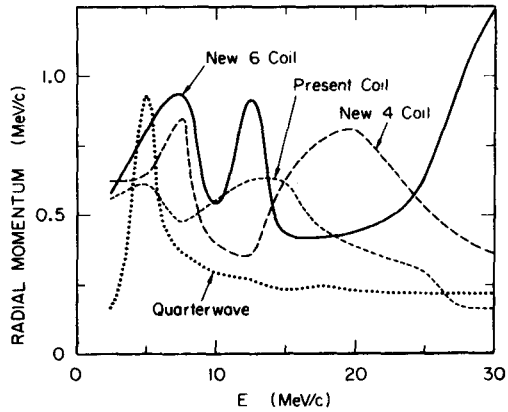

Fig. 3. Calculated radial momentum acceptance of focusing systems.

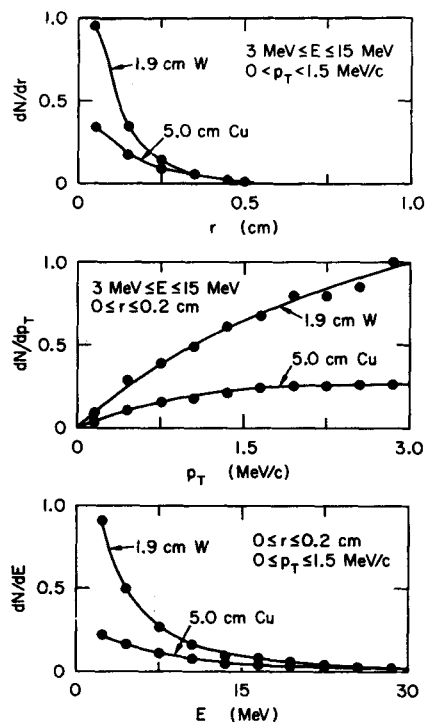

Fig. 4. Positron distribution in r, p_T, and E for 7 GeV incident electrons.

Table III. Positron Yields for Various Incident Electron Energies

Incident Energy	Yield	Yield/E	$\frac{\text{Yield/E}}{\left(\frac{\text{Yield at 7 GeV}}{\text{7 GeV}}\right)}$	Theoretical Multiplicity Divided by E and Normalized to 7 GeV
7 GeV	16.1 ± .8	2.3 %/GeV	1	1
1 GeV	2.7 ± .2	2.7 %/GeV	1.17	1.2
250 MeV	.83 ± .06	3.32%/GeV	1.44	1.44
80 MeV	.31 ± .03	3.88%/GeV	1.69	1.82

by incident energy scales reasonably well from the theoretical multiplicity given by Rossi,[5] divided by incident energy.

Acknowledgements

We wish to thank W. R. Nelson and W. B. Herrmannsfeldt for guidance in the use of their computer programs, and W. Brunk, K. Porzuczek and A. V. Lisin for carrying out the magnetic and mechanical design of the new solenoid. R. H. Helm and H. DeStaebler contributed with very helpful discussions during the study.

References

1. R. H. Helm, "Adiabatic Approximation for Dynamics of a Particle in the Field of a Tapered Solenoid," Stanford Linear Accelerator Center report SLAC-4 (1962).
2. R. H. Helm, The Stanford Two-Mile Accelerator, R. B. Neal, editor (W. A. Benjamin, New York, 1968).
3. R. L. Ford and W. R. Nelson, "The EGS CODE SYSTEM: Computer Programs for the Monte Carlo Simulation of Electromagnetic Cascade Showers," to be published as a Stanford Linear Accelerator Center report.
4. W. B. Herrmannsfeldt, "Electron Trajectory Program," Stanford Linear Accelerator Center report SLAC-166 (1973).
5. B. Rossi, High-Energy Particles, (Prentice-Hall, New York, 1952).

ДИСКУССИЯ

A.O.Hanson: What is the function of the quarter wave transformer in your system?

R.H.Miller: The "quarter wave transformer" is 1/2 a Larmour wavelength long so that it transforms the large initial radial momentum into a large radius and small radial momentum for a particular energy.

F.Netter: Do you believe that the quotation of 80 MeV e^- operation corresponds to the same problem of yield calculation? At such low energies, like at the Saclay linac, use of low energy e^+ beams (i.e. 100 MeV) is largely depending of energy acceptance and not only of spatial acceptance. Choice of RF phase for the 1-st and 2-nd accelerating sections can change drastically the yield in a given bandwidth of energy.

R.H.Miller: No, I certainly don't recommend a positron source like SLAC's for low energy positron beams because of the large initial energy spread. I made the calculation only to see how e^+ yields scale with energy.

H.Kumpfert: Were your calculations and yield measurements done for targets with different thickness or just one?

R.H.Miller: The targets were each different: appropriate for shower maximum at each energy.